

# Spectroscopic investigation (FT-IR, FT-Raman, NMR and UV), Molecular Docking and DFT analysis of 4-(Aminomethyl)Pyridine

**Thamarai. M**

*Department of physics, Kanchi mamunivar government Institute for post graduate studies and Research (Autonomous), pondicherry University, Pondicherry.*

**Jayasheela. K**

*Department of physics, Kanchi mamunivar government Institute for post graduate studies and Research (Autonomous), pondicherry University, Pondicherry.*

**Dr. S. Periandy**

*Department of physics, Kanchi mamunivar government Institute for post graduate studies and Research (Autonomous), pondicherry University, Pondicherry.*

## ABSTRACT

The compound was procured in the liquid form. The optimized structure of the molecule was obtained from Density Functional Theory method (DFT) with B3LYP/6-311++G(d,p) basis set. Conformational analysis was carried out by potential energy Scan technique to find minimum energy conformer for further studies. Structure of the molecule is analyzed in terms of bond length, bond angle. Atomic charge distribution has been investigated by Mulliken and Natural charge analysis. Vibrational frequencies were obtained from DFT computations and were compared with the experimental FT-IR and FT-Raman spectra to identify the functional groups. <sup>1</sup>H and <sup>13</sup>C NMR study of the compound was undertaken to study the chemical environment of the compound. Stability of the molecule and charge delocalization has been extracted from NBO analysis. UV-Vis spectrum was recorded to study the highest energy electronic transition. HOMO-LUMO analysis and MEP mapping were carried out. Molecular Docking studies for the molecule were computed to find the protein-ligand binding pose of the molecule to be used for pharmaceutical applications.

**Keywords:** FT-IR, FT-Raman, Docking analysis.

## 1. INTRODUCTION

Heterocyclic compounds finds importance in organic and biochemistry since they are predominate in the compounds used as drugs, agro chemicals and veterinary product [1]. Pyridine nucleus is present in many biological compounds which are used in drugs [2]. The biological importance of pyridine derivatives paved a way for the synthetic methods of construction of the pyridine ring and the formation of its derivatives [3,4]. Pyridine derivative is found to act as anesthetic agents, drugs for kind of certain brain diseases and also underpin analgesics for acute and chronic pain, common depression and even diabetic neuropathy. The picoline derivatives prepared from aminopyridine derivatives are confirmed to reduce cholesterol as well as anticancer and anti-inflammatory agents [5]. AminoPyridine is a foul smelling liquid aromatic amine and known for over 150 years. It is one among the first compounds for which liquid Raman scattering was studied [6] before the first detailed Infra -Red studies[7,8]. Amino Pyridine has a low molecular weight, relatively high volatility and moderate symmetry (C<sub>2v</sub>). Pyridine is a significant industrial compound therefore the quantitative analysis of pyridine can obviously be used for control of pollution and environmental effects, in biomass burning, orin other environmental problems [9]. Considering the various applications of the pyridine derivatives,

the compound 4-(aminomethyl) pyridine for which the DFT analysis combined with experimental spectroscopic studies have not been reported so far, is chosen for detailed structural and physicochemical analysis in the present study.

## 2. EXPERIMENTAL

4-(aminomethyl)pyridine was bought from Sigma–Aldrich Chemicals with spectroscopic grade and the spectra were recorded as such. The IR spectrum with application of Fourier transformation was performed in the range 500 to 4000  $\text{cm}^{-1}$  using Bruker IFS spectrometer. The resolution of the instrument is  $\pm 2 \text{ cm}^{-1}$ . Then the FT-Raman spectrum of the compound was recorded with FRA 106 Raman module in the same instrument, with Nd:YAG laser source operating at 1.064  $\mu\text{m}$  line widths with 200 mW power between the limits 3500–500  $\text{cm}^{-1}$  with an scanning speed of 30  $\text{cm}^{-1} \text{ min}^{-1}$  and the spectral width 2  $\text{cm}^{-1}$ . The NMR molecular chemical shift was recorded in  $\text{CDCl}_3$  (deuterated chloroform) solvent in the specific range of 20–200 ppm in the scanning interval of 20 ppm and also the UV-Visible spectrum was recorded in the range of 200–400 nm, with the scanning interval of 0.2nm, by using the UV-1700 series instrument.

## 3. COMPUTATIONAL

The entire set of quantum chemical computations were carried out using Gaussian 09 program [10] installed on a personal computer. By the use of DFT study the more stable conformer having the least potential energy was identified using potential energy surface scan. Geometrical analysis of the compound was evaluated. The harmonic vibrational frequencies were calculated, the corresponding wavenumbers were obtained using B3LYP with 6-311G (d, p) basis sets and the obtained frequencies were scaled by 0.956. The NMR molecular chemical shifts were calculated by GIAO method[11] with same functionals and basis sets. The electronic properties such as NBO, HOMO-LUMO and UV are calculated by TD-SCF methods. Mulliken charge distribution for all the entire molecular orbitals were charted, and their corresponding values are analyzed to identify the pharmaceutical applications of the molecule. The first order hyperpolarizability, dipole moment and chemical properties such as electrophilic index, electronegativity, global hardness and global softness of the title molecule were computed using B3LYP/6-311G (d, p) functionals and basis sets.

## 4. RESULTS AND DISCUSSION

### Conformational analysis

The conformational analysis of the molecule 4-(Aminomethyl)Pyridine was performed using B3LYP/6-311++G(d,p) hybrid functional and basis set by potential energy surface scan technique, varying the dihedral angle H16-C11-C12-H13 in steps of  $10^0$  for a complete rotation 0–360 $^0$ . The result of the scanning is shown graphically in Fig. 1 which clearly shows that one minimum at 180 $^0$  with energy 0.049 Hartree indicating the minimum energy conformer. Hence, the resulting structure serves as the high stable conformer of the compound and is the staggered configuration of the compound with less strain. The molecule shows one maximum energy point at 0 $^0$  with energy value 0.055 Hartree, which is the less stable conformer of the compound and represents the eclipsed configuration of the compound.

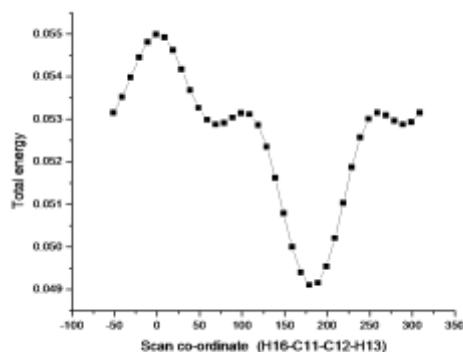


Fig. 1 Conformational analysis of 4-(Aminomethyl)Pyridine

### Molecular Analysis

The optimized structural parameters like (bond lengths and bond angles) of 4-(Aminomethyl)Pyridine was carried out using DFT/B3LYP method with 6-311++G(d,p) basis set [12] and are listed in Table 1. The structure of the molecule in stable configuration under optimized condition, with the numbering of atom, is given in Fig. 2. The structure shows five C-C, three C-N, four NH and six C-H bonds. CC single bond is in general expected to be around 1.50 Å and that of CC double bond around 1.34 Å. Wherein the covalent bond lengths between C-C in the ring is found to be 1.39 Å which indicates conjugation of bonds due to pi electrons delocalization of the p-orbitals of the carbon within the ring. The bond length C-N is also found within the ring to be 1.33Å, whereas the C11-N12 bond between methyl and amine group is observed as 1.46Å. This shows there is clear way of conjugation of electrons among the bonds which has reduced the CN bond lengths within ring. As seen in figure, the pyridine ring and methyl group are connected by the bond C3-C11 and the bond length value of this is 1.51 Å, which indicates this bond is slightly stretched because of the electrostatic repulsion as these two carbon atoms might be made positive due to the attached N atom on both ends.

The angles C4-C5-N6 and C2-C1-N6 inside the ring changes from 120° to 123° and 124° by the electron withdrawing nature of nitrogen atom. Due to the nitrogen insertion in the ring the bond angles N6-C1-H7 and N6-C5-H10 outside the ring decreases to 115° and 116° respectively. The bond angle C2-C3-C4 is decreased to a value of 117° due to the attachment of aminomethyl group at C3. The C11 is sp<sup>3</sup> hybridized and still the bond angles C3-C11-N12 and N12-C11-H15 changes to a value of 112° and 113° by the presence of higher electronegative nitrogen atom. These observations on bond angles clearly indicate that presence of N atoms have clearly altered the hybridization of the carbon atoms of the molecule, thus changed the structure appreciably.

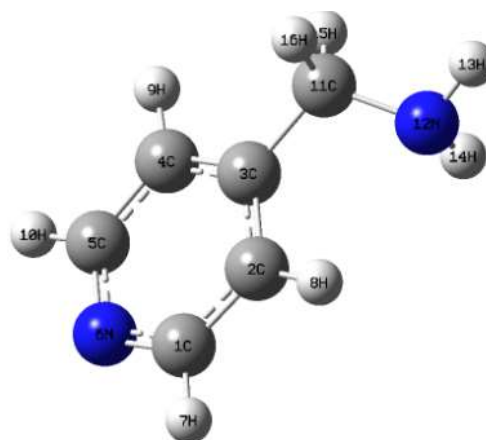


Fig.2. Structural analysis of 4-(Aminomethyl)Pyridine

**Table 1***Optimized Geometrical parameter of 4-(Aminomethyl)Pyridine at B3LYP/6-311++G(d,p)*

Bond Length (Å)	B3LYP/6-311++G (d,p)	Bond Angle (°)	B3LYP/6-311++G (d,p)
C1-C2	1.3932	C2-C1-N6	124.0238
C1-N6	1.3371	C2-C1-H7	120.0968
C1-H7	1.0875	H6-C1-H7	115.8794
C2-C3	1.3961	C1-C2-C3	119.0394
C2-H8	1.0835	C1-C2-H8	120.9027
C3-C4	1.3965	C3-C2-H8	120.0573
C3-C11	1.5151	C2-C3-C4	117.1772
C4-C5	1.3929	C2-C3-C11	121.8768
C4-H9	1.0864	C4-C3-C11	120.9304
C5-N6	1.3362	C3-C4-C5	119.3463
C5-H10	1.0875	C3-C4-H9	120.8341
C11-N12	1.4644	C5-C4-H9	119.8192
C11-H15	1.1006	C4-C5-N6	123.7294
C11-H16	1.0964	C4-C5-H10	120.2229
N12-H13	1.0138	N6-C5-H10	116.0468
N12-H14	1.0152	C1-N6-C5	116.6826
		C3-C11-N12	112.2353
		C3-C11-H15	108.6578
		C3-C11-H16	108.354
		N12-C11-H15	113.9289
		N12-C11-H16	107.2342
		H15-C11-H16	106.1094
		C11-N12-H13	110.8378
		C11-N12-H14	111.0371
		H13-N12-H14	107.5661

**Mulliken Population and Natural Atomic charge analysis**

To get an idea the way the charge is distributed over the atoms and molecular orbitals this atomic charge analysis is carried out, as these charges determine the dipole moment, polarizability and other reactive properties of the molecules. The distribution of positive as well as negative charges surrounding the atoms are vital to increase or decrease the bond length between them [13]. Two methods are employed to compute the atomic charges; one is Mulliken Population analysis (MPA) method and the other one is Natural atomic charge (NAC) method. The electronic charges of 4-(aminomethyl) pyridine thus calculated is presented in the table 2. The bar diagram representation on the result is shown in Fig.3.

From the table 2, it can be observed that the carbon atoms in the pyridine ring C1 and C5 which are attached to N directly, are predicted to be highly negative in MPA whereas slightly positive in NAC, among these predictions only the prediction by NAC can be possible as N can capture some of the electronic charges of these two carbons. The other three carbon atoms in the ring C2, C3 and C4 are expected to be equally negative as it is used to be in benzene. But C3 where the amino methyl group is attached is predicted to be positive in MPA and almost neutral in NAC, here also the prediction by MPA cannot be possible as the amino group is next to the methyl group. The C2 and C4 are found to be equally negative as expected, but these also are predicted to be highly positive and neutral in MPA which is also not justifiable. Hence, the NAC predictions are found to be reliable for all the carbon atoms inside the pyridine ring. In the case of methyl carbon atom C11, it is predicted to be highly negative taking into consideration the two hydrogen atoms in MPA but slightly negative in NPA, this is reasonable as this carbon atom is attached to N atom in the amino group. All the hydrogen atoms in the molecule are found to be equally positive in both the methods, except the hydrogens which are attached to the N atom in the amino group, they are found to be slightly over positive when compared to other H atoms.

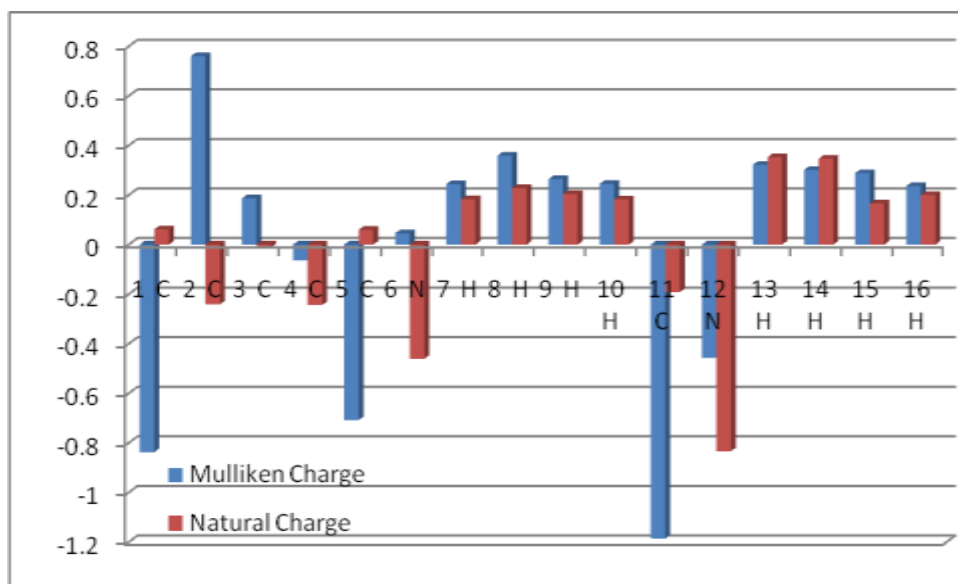


Fig. 3. Charge analysis of 4-(Aminomethyl)Pyridine

**Table: 2**

Charge analysis of 4-(Aminomethyl)Pyridine at B3LYP/6-311++G(d,p)

Atoms	B3LYP/6-311++G(d,p)	
	Mullikan Charge	Natural Charge

1 C	-0.83717	0.0616
2 C	0.759829	-0.2412
3 C	0.186463	-0.01164
4 C	-0.063	-0.24394
5 C	-0.70791	0.0595
6 N	0.045696	-0.46074
7 H	0.24383	0.18233
8 H	0.358598	0.22816
9 H	0.263993	0.204
10 H	0.245138	0.18215
11 C	-1.18542	-0.19158
12 N	-0.45757	-0.83347
13 H	0.321956	0.35234
14 H	0.301155	0.34656
15 H	0.288409	0.16582
16 H	0.236003	0.20012

### NMR Analysis

Nuclear magnetic resonance is a reliable technique that is used in many disciplines of scientific research, industries, medicine and for structural determination of biological macro molecules. Because of their higher sensitivity they are very valuable for structural investigations. The combined use of NMR and simulation methods by means of computer offers a powerful way to predict and interpret the structure of large bio molecules [14]. The NMR molecular chemical shift of the  $^{13}\text{C}$  and hydrogen atoms of the molecule are determined by the use of same functional and basis set B3LYP/6-311++G(d,p) along with gauge-independent atomic orbital(GIAO) functional which is meant for it. Experimentally, the  $^1\text{H}$  and  $^{13}\text{C}$  chemical shift were measured in DMSO solution for comparison. Table 3 shows the computed values in gaseous and solvent phase. The  $^1\text{H}$  and  $^{13}\text{C}$  theoretically calculated chemical shift of the compound is shown in Fig 4 & 5.

Unsaturated carbons give signals with chemical shift values ranging from 100 to 200 ppm.  $^{13}\text{C}$  NMR spectra shows signal in the range 120 -130 ppm for carbon atoms in benzene. The 1C and 5C in the pyridine ring shows a chemical shift value of 148 ppm which is higher than the expected value, it confirms the positive charge prediction for these two atoms by NAC method due to the attachment of N atom. It shows that the chemical environment is disturbed by the presence of nitrogen atom. Almost the same chemical shift value 150 ppm is observed for 3C where the substitution amino methyl group is attached but, this observation slightly deviates from the prediction of even NAC. Therefore the magnetic field experienced externally by carbon nuclei is varying by the electronegativity of the atoms attached to them. Therefore electronegative substituents attached to carbon decrease the local diamagnetic shielding in the vicinity of the attached proton and de-shield them. The higher the electronegativity of the substituent atom the more it de-shields proton and higher is the chemical shift. The shift of C2 and C4 are found be in the expected line 124 ppm as correctly predicted by NAC in the

charge analysis. The chemical shift of the methyl carbon C11 (45 ppm) also support the charge prediction by NAC.

Commonly the hydrogen attached to a nearby electron withdrawing group decreases the electronic shielding and shifts the resonance of the attached proton to the higher frequency value. On the other hand the electron donating group increases the electronic shielding and thereby shifts the resonance of the proton to a lower frequency value [15]. In our molecule there are eight hydrogen atoms for which the chemical shifts theoretically and experimentally are presented in the table 3. Among the eight atoms 4 hydrogen atoms are located in the aromatic ring and the remaining to the aminomethyl group. The 9H atom is influenced by the nearby attachment group. The 15H and 16H which are attached to the amino group show the lowest values nearly 1 ppm which shows they get shielded instead of deshielding.

**Table. 3.**

**Calculated  $^1\text{H}$  and  $^{13}\text{C}$  NMR Chemical shifts (ppm) of 4-(Aminomethyl)Pyridine at B3LYP/6-311++G(d,p)**

Atom	Gas	CDCl <sub>3</sub>	Experimental
	B3LYP/6-311++G(d,p) GIAO (ppm)	B3LYP/6-311++G(d,p)GIAO (ppm)	
1 C	155.2	154.7	148.0
2 C	124.8	125.4	120.5
3 C	156.4	159.2	150.9
4 C	124.8	126.2	120.5
5 C	154.2	154.1	148.0
11 C	49.0	48.85	43.5
7 H	8.5	8.4	7.7
8 H	7.6	7.7	7.7
9 H	6.9	6.8	6.4
10 H	8.3	8.3	7.7
13H	0.5	0.8	1.0
14H	0.1	0.3	1.0
15H	3.8	3.9	3.0
16H	3.6	3.7	3.0

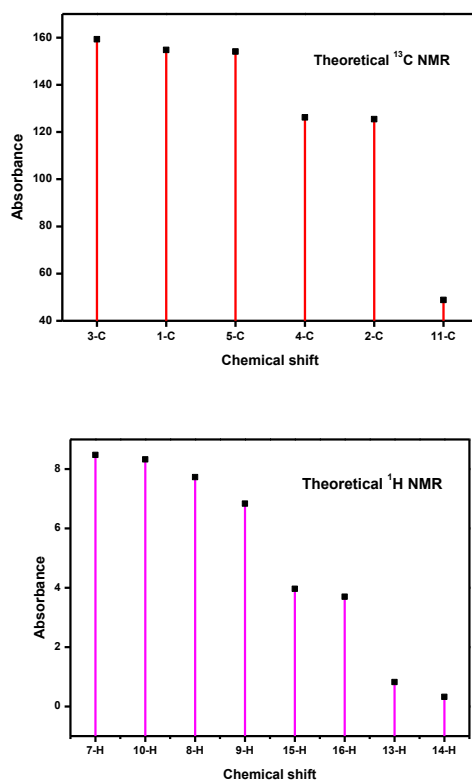


Fig. 4. Theoretical <sup>13</sup>C and <sup>1</sup>H NMR of 4-(Aminomethyl)Pyridine

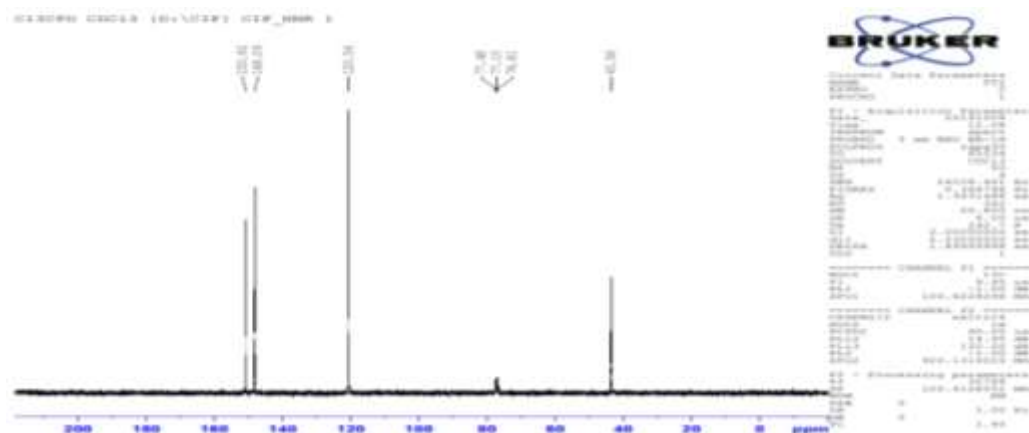


Fig. 5. Experimental <sup>13</sup>C and <sup>1</sup>H NMR of 4-(Aminomethyl)Pyridine

### Vibrational Analysis

Quantum chemical simulations helped in calculating the vibrational frequencies, along with the IR intensities and the Raman activity. The computed frequencies were scaled with constant scaling factor and is in good agreement with the observed data. The chosen molecule has 16 atoms. Therefore the molecule possess 42 possible modes of vibration and all the modes of vibration are observed in IR and as well as Raman spectra. The experimental wave number value and calculated wave number value and its corresponding assignments made using PED are represented in Table 4. The theoretical and



experimental spectra of FT-Raman and FT-IR for the molecule are represented in the Fig. 6 and 7. The experimental frequency values are correlated with the theoretically obtained data by scaling the harmonic frequencies of the calculated wavenumbers. For this a numerically calculated common scaling factor of 0.956 was used for the entire calculation.

### C-H vibrations

The characteristic vibrational for the C-H stretching mode of the hetero aromatic molecules appear in the wavelength range  $3000-3100\text{ cm}^{-1}$  [16]. The C-H stretching vibration for the molecule 4-aminomethyl pyridine was observed at  $3048\text{ cm}^{-1}$  and  $2912\text{ cm}^{-1}$  in Raman spectrum and the corresponding theoretical wavenumbers are  $3153\text{ cm}^{-1}$  and  $3097\text{ cm}^{-1}$ . In IR spectrum it is noticed at  $2970\text{ cm}^{-1}$  and  $2920\text{ cm}^{-1}$ . The corresponding theoretical scaled wavenumbers is at  $3118\text{ cm}^{-1}$  and  $3102\text{ cm}^{-1}$ . The experimental values are less than the theoretically calculated values since the C-H stretching vibration are affected by the substitution. In the methylene group C-H stretching, asymmetric  $\text{CH}_2$  stretching vibration is observed within the wavenumber region  $3000-2900\text{ cm}^{-1}$  whereas the  $\text{CH}_2$  symmetric stretch is shown in the region  $2900-2800\text{ cm}^{-1}$ . The bands at  $2888\text{ cm}^{-1}$  and  $2854\text{ cm}^{-1}$  in FT-IR spectrum are assigned to  $\text{CH}_2$  symmetric stretching vibrations. The theoretically calculated value is  $2988$  and  $2921\text{ cm}^{-1}$ . The red shifting of the methylene stretching wave number is due to the electronic charge surrounding it. The C-H bond in-plane bending vibrations occurring in the region  $1400-1200\text{ cm}^{-1}$  is useful for characterization purpose [17]. The C-H in-plane vibrations computed at  $1350, 1239, 1207, 1168, 1096, 1074\text{ cm}^{-1}$  shows good agreement with FT-IR spectral region at  $1336, 1152$  and  $1066\text{ cm}^{-1}$  and as well as FT-Raman spectral region at  $1098$  and  $1066\text{ cm}^{-1}$ .

### C-C vibration

The ring C-C stretching vibrations usually occur in the wavenumber region limits  $1625-1430\text{ cm}^{-1}$  [18]. For six membered aromatic ring (benzenes and pyridines) there are two or three vibrational bands appearing in this region arising due to ring vibrations and the strongest vibration being about  $1500\text{ cm}^{-1}$ . The aromatic C-C stretching are observed at  $1688, 1605, 1561$  and  $1472\text{ cm}^{-1}$  in FT-IR and  $1600, 1558, 1494$  in FT-Raman spectrum while the DFT calculation gives the C-C stretching modes at  $1684, 1614, 1579, 1508$  and  $1487\text{ cm}^{-1}$ . It is observed that the experimental value very well coincides with the computed data as well as the literature value. The planar ring deformation mode is observed at  $1000\text{ cm}^{-1}$  in FT-IR spectrum and the DFT calculated value is  $1048\text{ cm}^{-1}$  are in good agreement.

### Vibrations of the $\text{NH}_2$ group

In the earlier literature survey it has been described that amines shows absorption bands in the wavenumber region  $3350-3150\text{ cm}^{-1}$ . The absorption wavenumber within this range depends on the degree of hydrogen bonding and so upon the physical nature of the sample or polarity of the sample as well [19]. The vibrational band arising due to N-H stretching is sharp and weak than those due to O-H stretching vibrations which make easy identification of the band [20]. The band at  $3363\text{ cm}^{-1}$  and  $3258\text{ cm}^{-1}$  is due to N-H antisymmetric and symmetric stretching vibrations. The corresponding theoretical scaled value is found at  $3528\text{ cm}^{-1}$  and  $3447\text{ cm}^{-1}$  which shows that experimental value is in good coincidence with the theoretical value. The vibrational band at  $993$  and  $985\text{ cm}^{-1}$  in Raman spectrum is attributed to NH bending vibration whose value coincides with the DFT calculated value of  $995$  and  $984\text{ cm}^{-1}$ .

### C-N vibrations

The C-N bond stretching vibration is usually mixed with other vibrational bands and assigned in the wave number range  $1382-1266\text{ cm}^{-1}$  [21]. In our present molecular study the computed values at  $1305, 1252$  and  $1239\text{ cm}^{-1}$  is supported by the presence of experimental band at  $1307, 1222$  in FT-IR and  $1275$  in FT-Raman spectrum.

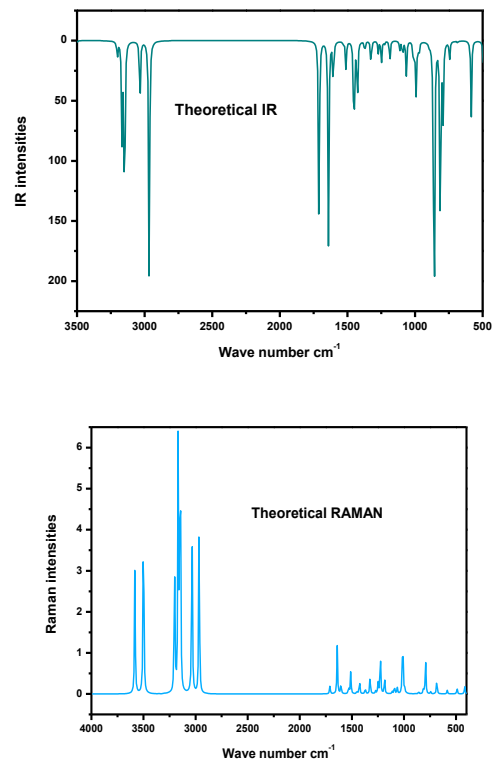


Fig. 6.Theoretical IR and RAMAN Spectra4-(Aminomethyl)Pyridine

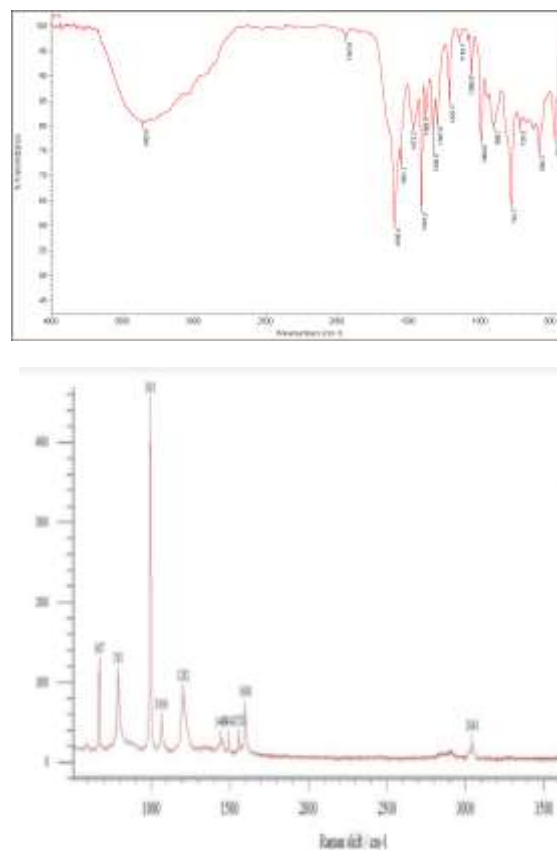


Fig. 7.Experimental IR and RAMAN Spectra4-(Aminomethyl)Pyridine

**Table 4.**  
**Experimental FT-IR, FT-Raman and Calculated 4-(Aminomethyl)Pyridine at B3LYP/6-311++G(d,p) levels of vibrational frequencies (cm<sup>-1</sup>)**

No	frequencies (cm <sup>-1</sup> )				Assignment	VEDA
	Observed		Calculated			
	IR	Raman	Un scaled	Scaled		
1	3363		3582	3528	v NH	v NH 63
2	3258		3500	3447	v NH	v NH 36
3		3048	3202	3153	vCH	v CH 97
4	2970		3166	3118	vCH	v CH 75 + 23
5	2920		3150	3102	vCH	v CH 93
6		2912	3145	3097	vCH	v CH 21 + 75
7	2888		3034	2988	vCH	v CH 97
8	2854		2966	2921	vCH	v CH 97
9	1688		1710	1684	v CC	β HNH 86
10	1605	1600	1640	1614	v CC	v CC 17 + 17 + β CCC 12
11	1561		1604	1579	v CC	v CC 40 + β CCN 13
12		1558	1531	1508	v CC	β HCN 24 + HCC 10 + 13 + HCN 22
13	1472	1494	1510	1487	v CC	β HCH 81
14	1418	1415	1451	1429	β NH	v CC 11 + 13 + β HCN 18
15	1383		1426	1404	β NH	β HCN 15 + 10 + τ HNCH 21
16	1336		1371	1350	β CH	β HCN 16 + 17 + HCC 15 + 13 + 12
17	1307		1325	1305	v CN	β HCN 41
18		1275	1272	1252	v CN	v NC 29 + CC 23 + β HCN 12
19	1222		1248	1239	v CN	v NC 16 + CC 10 + β HCN 19 + 23
20		1202	1226	1207	β CH	v CC 30 + HCC 10 + CCC 14
21	1152		1186	1168	β CH	β HCN 33 + τ HNCH 32
22		1098	1113	1096	β CH	v CC 18 + 25 + β HCC 20
23	1066	1066	1091	1074	β CH	β CCN 10 + 16 + HCC 29 + 14
24	1000		1064	1048	β CC	v NC 26 + 74
25		993	1011	995	β NH	v NC 18 + 19 + β CCN 11 + 15 + CNC 14

26		985	999	984	$\beta$ NH	$\tau$ HCCH 64
27		980	990	975	$\beta$ CN	$\beta$ HCN 14 + $\tau$ HCCH 18 + HNCH 24
28	909		971	956	$\beta$ CN	$\tau$ HCCH 19
29		886	893	879	$\beta$ CN	$\gamma$ CCNH 49 + $\tau$ HCCN 34
30		855	859	846	$\beta$ CNC	$\gamma$ NHCH 47
31	791		813	800	$\beta$ CNC	$\gamma$ NHCH 18 + CCNH 18 + $\tau$ HCCN 36
32		788	792	780	$\beta$ CCH	$\nu$ CC 20 + $\beta$ CNC 32 + $\tau$ HCCH 59
33	728		744	732	$\beta$ CCH	$\tau$ CCNC 31 + $\tau$ CCCC 47
34		667	684	673	$\beta$ CCH	$\beta$ CCN 50 + 23
35	594		584	575	$\beta$ CCH	$\beta$ CCC 29 + CCN 29
36	484		490	482	$\beta$ CCH	$\beta$ CCC 15 + $\tau$ CCNC 37 + CCCN 11
37			417	410	$\beta$ CCH	$\nu$ CC 13 + $\beta$ CCC 26 + CCN 18
38			390	384	$\beta$ CCC	$\tau$ CCNC 72 + CCCC 14
39			272	267	$\beta$ CCC	$\tau$ HNCC 57 + CCCC 10
40			245	241	$\beta$ CCC	$\beta$ CCC 48 + CCN 17
41			167	164	$\beta$ CCN	$\beta$ CCN 12 + $\tau$ CCCC 61
42			56	55	$\beta$ CCN	$\tau$ CCCN 94

$\nu$ -stretching,  $\delta$  -in-plane bending,  $\gamma$ -out-of-plane bending,  $\sigma$ -scissoring,  $\rho$ -rocking,  $\tau$ -twisting,  $\delta$ ring-in-plane bending ring,  $\gamma$ ring-out-of-plane bending ring.

### NBO Analysis

Natural bonding Orbital Analysis is a resourceful method for studying intra and inter-molecular interaction among bonds and for investigating charge transfer or conjugative interaction in molecular system. In Weinhold's NBO calculation, hyperconjugation has a stabilizing effect which is due to movement of electrons from bonding Lewis type NBO to Non-Lewis type NBO when these molecular orbitals are aptly oriented.

NBO analysis provides the possible natural lewis structure of  $\Psi$ . This is due to the fact that all orbital details are accounted mathematically for inclusion of the highest possible percentage of the electron charge density. The second order Fock matrix was carried out for evaluating the donor acceptor interaction [22]. For each electron donating NBO (i) and electron accepting NBO (j) the stabilization energy  $E^{(2)}$  associated with the electron delocalization  $i \rightarrow j$  is estimated as [23]

$$E_2 = \Delta E_{ij} = q_i \frac{F(i,j)^2}{E_i - E_j}$$

Larger the  $E^{(2)}$  value, more intensive is the interaction between donors and acceptors. Parameter such as occupancy, electron donors and acceptors, stabilization energy etc., are extracted from the NBO Gaussian output file, computed by B3LYP/6-311++G(d,p) method are noted in Table 5. The resonance of the molecule is related with the most significant electronic interaction  $n \rightarrow \pi^*$ . The most important interaction energy in the molecule is electron donating from N6 (1) to the antibonding

C<sub>4</sub>-C<sub>5</sub> with stabilization of 9.14KJ/mol. The same N<sub>6</sub> (2) donating electron to antibonding C<sub>1</sub>-C<sub>2</sub> leads to the stabilization of 9.12KJ/mol. The second order perturbation energies corresponding to the hyper conjugative interaction of pyridine ring such as;  $\pi_{C_2-C_3} \rightarrow \pi^*_{C_1-N_6}$  (29.02 Kcal/mol),  $\pi_{C_1-N_6} \rightarrow \pi^*_{C_4-C_5}$  (27.07 Kcal/mol),  $\pi_{C_4-C_5} \rightarrow \pi^*_{C_2-C_3}$  (23.44 Kcal/mol),  $\pi_{C_2-C_3} \rightarrow \pi^*_{C_4-C_5}$  (17.49 Kcal/mol),  $\pi_{C_1-N_6} \rightarrow \pi^*_{C_1-N_6}$  (16.55 Kcal/mol),  $\pi_{C_1-N_6} \rightarrow \pi^*_{C_1-C_3}$  (13.01 Kcal/mol), are considerably large. The aforesaid hyper conjugative interactions contribute to the electronic transitions of the pyridine ring in the molecule.

The resonance of the molecule can be related to the most significant interaction  $n \rightarrow \sigma^*$ . The energies of electron donating from N<sub>6</sub> atom of the donor group to the antibonding acceptor  $\sigma^*_{C_4-C_5}$  (9.14 Kcal/mol),  $\sigma^*_{C_1-C_2}$  (9.12 Kcal/mol),  $\sigma^*_{C_5-C_{10}}$  (4 Kcal/mol) and  $\sigma^*_{C_1-H_7}$  (3.99 Kcal/mol) and further N<sub>12</sub> to  $\sigma^*_{C_{11}-H_{15}}$  (9.14 Kcal/mol), N<sub>12</sub> to  $\sigma^*_{C_{11}-H_{15}}$  (9.14 Kcal/mol), leads to less stabilization.

**Table 5.**

**Natural bonding analysis of 4-(Aminomethyl)Pyridine at B3LYP/6-311++G(d,p) levels**

Donor	Type of bond	Occupancy	Acceptor	Type of bond	Occupancy	Energy E(2) kcal/mol
C 2 - C 3	$\pi$	1.629	C 1 - N 6	$\pi^*$	0.381	29.02
C 1 - N 6	$\pi$	1.714	C 4 - C 5	$\pi^*$	0.304	27.07
C 4 - C 5	$\pi$	1.646	C 2 - C 3	$\pi^*$	0.327	23.44
C 2 - C 3	$\pi$	1.629	C 4 - C 5	$\pi^*$	0.304	17.49
C 4 - C 5	$\pi$	1.646	C 1 - N 6	$\pi^*$	0.381	16.55
C 1 - N 6	$\pi$	1.714	C 2 - C 3	$\pi^*$	0.327	13.01
N 6	n	1.999	C 4 - C 5	$\sigma^*$	0.025	9.14
N 6	n	1.999	C 1 - C 2	$\sigma^*$	0.025	9.12
N 12	n	1.957	C 11 - H 15	$\sigma^*$	0.031	7.32
C 11 - H 16	$\sigma$	1.965	C 2 - C 3	$\pi^*$	0.327	4.92
C 1 - H 7	$\sigma$	1.982	C 5 - N 6	$\sigma^*$	0.015	4.72
C 5 - H 10	$\sigma$	1.982	C 1 - N 6	$\sigma^*$	0.016	4.68
C 2 - H 8	$\sigma$	1.978	C 1 - N 6	$\sigma^*$	0.016	4.38
C 2 - H 8	$\sigma$	1.978	C 3 - C 4	$\sigma^*$	0.021	4.35
C 4 - H 9	$\sigma$	1.979	C 5 - N 6	$\sigma^*$	0.015	4.29
C 4 - H 9	$\pi$	1.646	C 2 - C 3	$\sigma^*$	0.024	4.2
C 11 - H 15	$\sigma$	1.983	C 2 - C 3	$\sigma^*$	0.024	4.11
N 6	n	1.999	C 5 - H 10	$\sigma^*$	0.023	4
N 6	n	1.999	C 1 - H 7	$\sigma^*$	0.023	3.99

### UV Visible Analysis

The UV-Visible spectral analysis of the compound has been studied theoretically in DMSO and gas phase. The excitation energies and oscillator strengths of 4-(aminomethyl) pyridine are computed using B3LYP with function and 6-311++G (d,p) basis set along with TD-SCF method [24]. The excitation energies, oscillator strength (f) and absorption wavelength ( $\lambda$ ) and HOMO-LUMO contributions are also presented in Table.6. The UV- theoretical and Experimental spectra are presented in Fig.8. As per Frank-Condon rule, the maximum absorption peak corresponds to vertical excitation. TD-SCF/B3LYP/6-311++G(d,p) predicts one highly intense electronic transition at 224 nm with oscillator strength 0.0439 in DMSO phase, the experimental spectrum also show peak at this wavelength but the maximum peak in experimental spectrum corresponds to the first transition at 259 nm whose theoretical value 250 nm with oscillator strength  $f=0.0045$ . Theoretically another peak is expected at 191nm with oscillator strength is 0.0166, but this peak is not observable in experimental spectrum. In experimental spectrum, there is a continuous peak upto 800 nm which shows all the  $n - \sigma^*$  and  $n - \pi^*$  predicted theoretically in NBO have occurred experimentally, though theoretically they are less favoured.

In gas phase, the peaks are expected at wavelengths 239, 230 and 216 nm respectively which is different from those of solvent phase that shows the solvent has the influence on the favorability of the electronic transitions in the molecule.

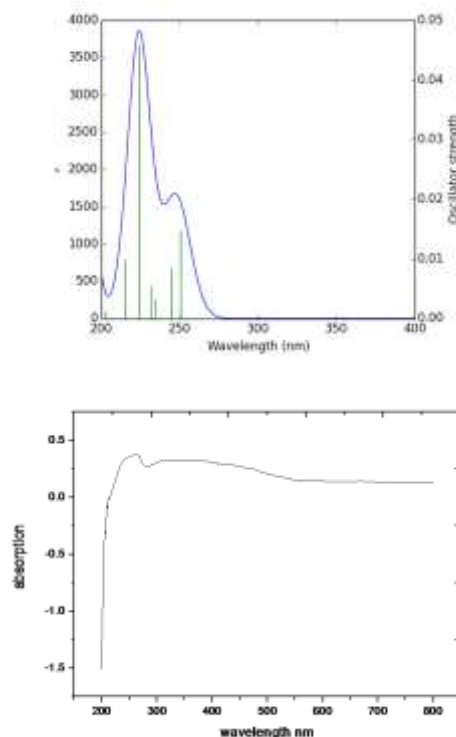


Fig. 8. Theoretical and Experimental UV Spectra 4-(Aminomethyl)Pyridine

Table 6.

## Electronic Absorption Wavelengths of 4-(Aminomethyl)Pyridine at B3LYP/6-311++G(d,p)

Gas phase				
$\lambda$ (nm)		E (eV)	(f)	Major Contribution
256.3		4.8357	0.0043	H-1->LUMO (58%)
242.4		5.1146	0.0000	H-1->L+1 (61%)
239.1		5.1855	0.0184	H-1->LUMO (37%)
230.2		5.3856	0.0190	H-3->L+1 (14%)
221.3		5.6018	0.0080	H-1->L+2 (12%)
216.8		5.7185	0.0163	H-2->LUMO (11%)
204.4		6.0646	0.0021	H-1->L+2 (70%)
202.9		6.1107	0.0012	H-3->LUMO (28%)
200.3		6.1898	0.0020	H-3->LUMO (23%)
195.7		6.3345	0.0081	HOMO->L+3 (70%)
Solvent phase (DCM)				
Theo $\lambda$ (nm)	Exp.	E (eV)	(f)	Major Contribution
250.3	259	4.9528	0.0147	H-2->LUMO (12%)
244.6		5.0683	0.0085	H-2->LUMO (85%)
234.5		5.2854	0.0033	H-2->L+1 (28%)
231.4		5.3563	0.0054	H-2->L+1 (67%)
224.1		5.5325	0.0459	H-3->L+1 (18%)
215.1		5.7623	0.0098	HOMO->L+2 (85%)
202.6		6.1192	0.0012	H-3->LUMO (47%)
193.6		6.4025	0.0049	HOMO->L+2 (12%)
192.2		6.4500	0.0069	H-1->L+2 (83%)
191.0		6.4901	0.0166	H-2->L+2 (23%)

## Frontier Molecular Orbital (FMO) Analysis

Useful information on the electronic structures of molecule can be got from the molecular orbital analysis. The LUMO, HOMO also called as the frontier molecular orbitals and the difference in energy level between them is called as the energy band gap. This energy gap is used to find molecular

electrical transport property, chemical reactivity, optical polarizability, chemical hardness and softness of the molecule [25]. The HOMO means the ability of an orbital to donate an electron and LUMO means the ability to accept an electron. It is predictable that larger is the energy band gap of the compound, lower is the chemical and photochemical reactivity process which is mostly due to electron transfer [26,27].

The energy of highest occupied molecular orbitals and lowest unoccupied molecular orbital with B3LYP method 6-311++G(d,p) basis set was calculated and are represented in table 7. The values are encapsulated as follows: HOMO (-0.257 eV) and LUMO (0.008 eV) and the energy gap of the optimized molecule is -0.265eV. The 3D plots of HOMOs and LUMOs computed for the molecule 4-(aminomethyl) pyridine is shown in Fig.9. In the figure red section is positive and negative one is green. It also shows that the HOMO and LUMO is localized on the ring itself. The electronegativity which is the measure of attraction of electron by an atom has value of 0.124eV. The chemical hardness of the molecules is 0.132eV and softness is 0.531eV.

**Table 7**

**Calculated energy value of the 4-(Aminomethyl)Pyridineat B3LYP/6-311++G(d,p) method.**

Parameters	Gas
$E_{\text{HOMO}}$ (eV)	-0.257
$E_{\text{LUMO}}$ (eV)	0.008
$\Delta E_{\text{HOMO-LUMO gap}}$ (eV)	-0.265
Electronegativity ( $\chi$ )	0.124
Global hardness ( $\eta$ )	0.132
Global softness (S)	0.531
Chemical potential	0.531

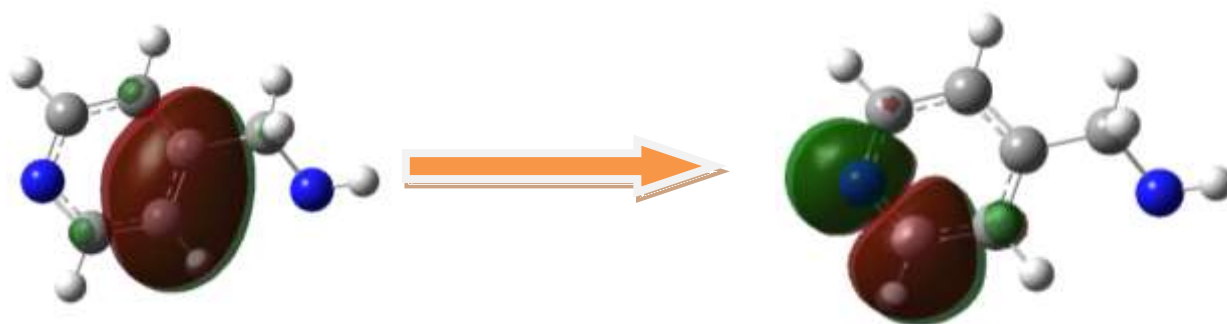


**Fig. 9.HOMO- LUMO picture of 4-(Aminomethyl)Pyridine**

### Molecular Electrostatic Potential Mapping

Molecular electrostatic potential (MEP) mapping is connected to the electronic charge density distribution. This method of mapping is useful for the identification of electrophilic and nucleophilic chemical reaction sites and also in study of biological recognition as well as hydrogen-bonding interactions. The reactive sites of the molecule have been investigated by MEP map at B3LYP/6-311++(d,p) using optimized geometry is shown in Fig.10. The red(negative) regions represent electrophilic reactivity and blue(positive) regions to nucleophilic reactivity. From MEP map the



negative sites lie on the amine group attached to the ring and the positive site lies near the nitrogen atom of the ring. The molecular electrostatic potential (MEP) surface indicates electron and nuclei distribution, molecular size, shape and dipole moments of the molecule. The potential increases in order red<orange<yellow<green<blue. The colour code of the map is in the range between  $-5.229e-2$  a.u. to  $5.229e-2$  for this compound. Here blue indicates the strongest attraction and red indicates the strongest repulsion. From the map it is clear that 6N atom indicates repulsion and all other atoms indicates neutral electrostatic potential. The advantage of the MEP is that it gives a collective picture of the localization of the electrons and its ability to get polarized, with reactive possibilities along with size and shape of the molecule [28].

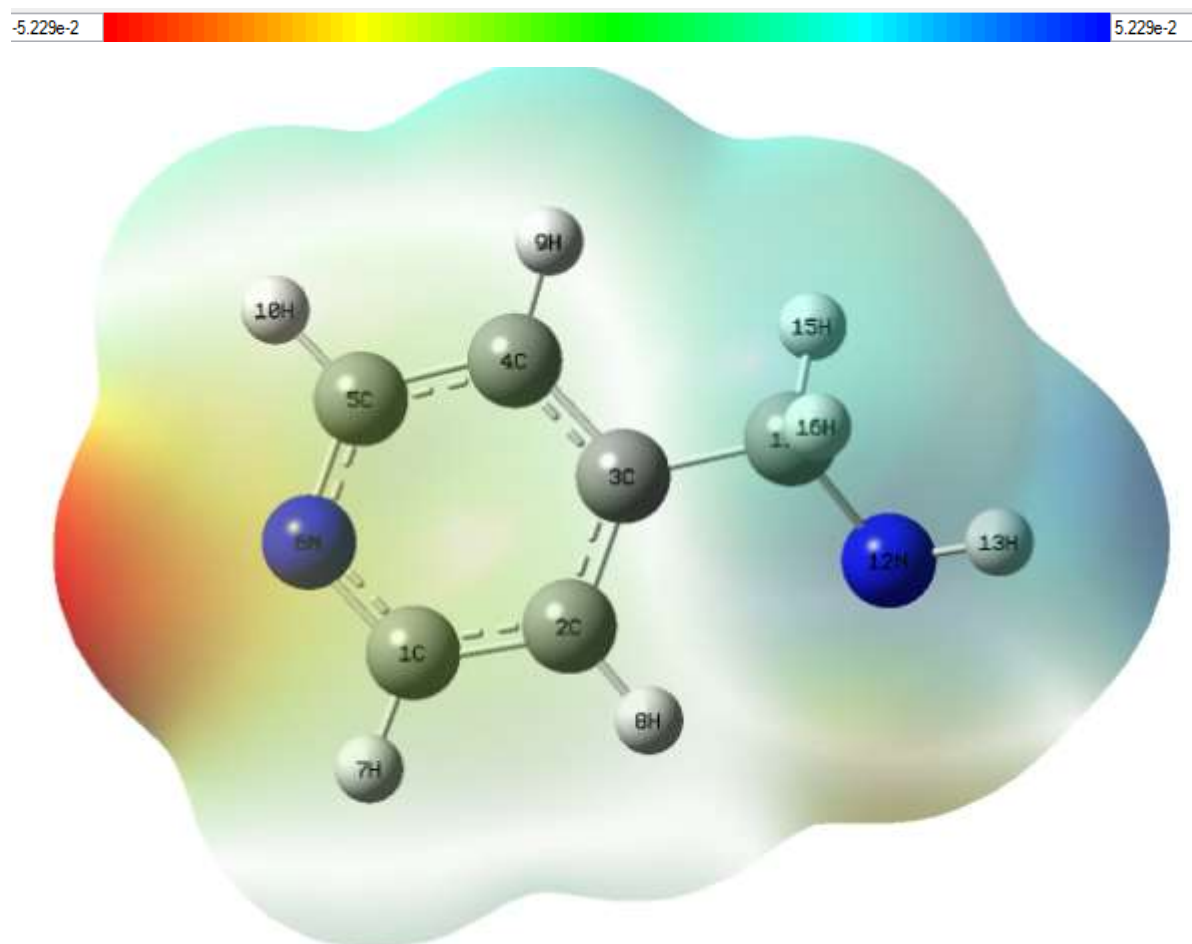


Fig. 10.MEP analysis of 4-(Aminomethyl)Pyridine

### Molecular Docking

Molecular docking is a powerful approach for predicting the molecular mechanism of protein - ligand interactions, through which the molecule can bind to a macro molecule, particularly proteins like bacteria, virus etc that change its dynamics. Auto Dock suite 4.0 [29] software is applied to get insight into probable protein-ligand interactions and to identify the binding affinity of the molecules. For docking the ligand was prepared by minimizing its energy at B3LYP/6-311++G (d,p). Hydrogen atoms are added to the target protein and Kollaman atomic charges was calculated. Water molecules and other co-crystallized agents were removed. Lamarckian genetic algorithm (LGA) is used for molecular docking analysis. The binding protein of the target protein was specified using grid size  $84 \times 84 \times 84 \text{ \AA}^3$  with the aid of Autogrid. Docked conformation which has the lowest binding energy was chosen to investigate the mode of binding. The results of docking; residues, hydrogen bonds and total number of bonds are noted in Table .8. The bond lengths are shown in Fig. 11.

Molecular docking of the ligand with the protein 3NUO(HIV-I) showed that three hydrogen bonds were formed between the side chain of GLU161 with the nitrogen atom of the ring and hydrogen atom of the amine group with a backbone of GLU95 and ALU93. It displays the ability to form hydrophobic interactions with the central residues in the active site of the enzyme. This validates that, the ligand displays more potent inhibitory activity against the enzyme protease and could be developed as a useful anti HIV-I drug.

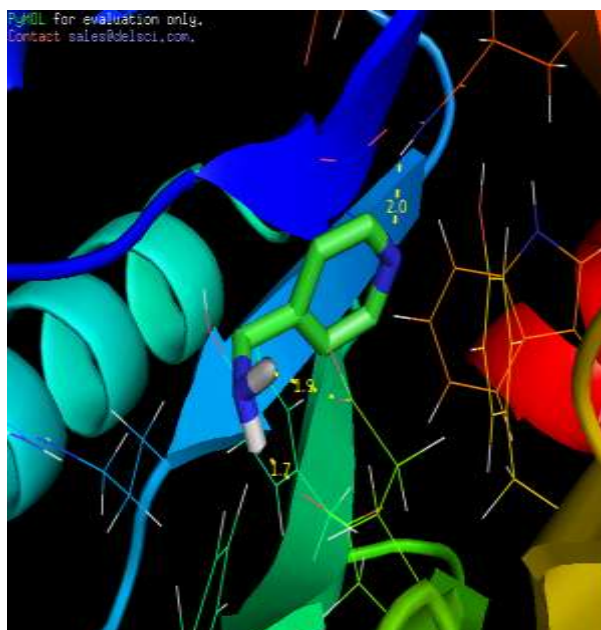


Fig. 11. Binding pose in 4-(Aminomethyl)Pyridine

**Table 8 Docking analysis of 4-(Aminomethyl)Pyridine**

Protein ID	Bond Residue	Distance (Å)
3NUO	GLU 95	1.9
	ALU 93	1.7
	GLU 161	2.0

## 5. CONCLUSION

The structural analysis shows that CC bond length within the ring is 1.39 Å and the bond length CN is also 1.33Å, they are neither double bond value nor single bond value. This shows there is clear conjugation of electrons within the ring. The bond angles around the carbon atoms within the ring are not found equal to 120°, similarly at the chain not 109°, these values implies that the presence of N atom could dismantle the conventional hybridization value of carbon atoms. In the charge analysis, the prediction of the charges by NAC method was found to be reliable when compared to MPA method for all the carbon and hydrogen atoms. The carbon atoms which are connected to N are found positive. These results are confirmed by the NMR chemical shift values; the 1C and 5C in the pyridine ring shows a chemical shift value of 148 ppm which is higher than the expected value, it confirms the positive charge prediction for these two atoms by NAC method due to the attachment of N atom. Almost the same chemical shift value 150 ppm is observed for 3C where the substitution amino methyl group is attached. This is not predicted by the charge analysis. The vibrational bands CH and CC of pyridine ring confirmed the presence of conjugation within ring. The presence of NH bands at 3363

$\text{cm}^{-1}$  and  $3258\text{cm}^{-1}$  indicate they can form intermolecular hydrogen bonds. The NBO analysis shows that  $n \rightarrow \pi^*$  bonds are not possible in this compound. The prominent transitions in this molecular are  $\pi \rightarrow \pi^*$  transitions in the pyridine ring and no transition is possible in amino methyl group. The peak expected at experimental spectrum is  $\pi\text{C}_2\text{-C}_3 \rightarrow \pi^*\text{C}_1\text{-N}_6$  (29.02 Kcal/mol), but there is a continuous peak upto 800 nm which shows all the  $n - \sigma^*$  transition predicted theoretically in NBO have occurred experimentally. Through docking study, it is found that the molecule binds with the protein 3NUO(HIV-I) by three hydrogen bonds, with the nitrogen atom of the ring and hydrogen atom of the amine group, thus the compound could be used to develop anti HIV-I drug.

## REFERENCES

1. T.L. Gilchrist, Heterocyclic Chemistry, 3th ed., Longman, Harlow, 1997, pp. 1-8.
2. J.A. Joule, K. Mills, Heterocyclic chemistry, fifth ed., Wiley Blackwell, Oxford, 2010, pp.645-664.
3. M. Balasubramanian, J.G. Keay, Compr. Heterocycl. Chem. II 5 (1996) 245-300.
4. C.DJohnson, Compr. Heterocycl. Chem. II 5 (1996) 1-35. 5. G. Jones, Compr. Heterocycl. Chem. II 5 (1996) 167-243.
5. S.P. Jose, S. Mohan, Spectrochim. Acta A 64 (1) ( 2006) 240.
6. Venkateswaran, S. On the Raman effect in liquid pyridine. J PhysChem 1930;34:145-52
7. Corrsin L, Fax BJ, Lord RC. The Vibrational Spectra of Pyridine and Pyridine- $\text{d}_5$ . J ChemPhys 1953; 21:1170-76.
8. Cook GL, Church FM. Correlations of the Infrared Spectra of some Pyridines. J PhysChem 1957;61:458-62
9. Johnson TJ, Disselkamp RS, Su YF, Fellows RJ, Alexander ML, Driver CL. Gas-phase Hydrolysis of  $\text{SOCl}_2$ : Implications for its Atmospheric Fate. J PhysChem A 2003;107:6183-90
10. R.P. Hirschmann, et al., Spectrochim. Acta A 30 (1974) 1293.
11. R. Ditchfield, Mol.Phys.27 (1974) 789. K. Wolinski, J.F. Hinton, P. Pulay, J. Am. Chem. Soc. 112 (23) (1990) 8251.
12. J .H.Vander Mass and E.T.G.Lutz, Spectrochimca Acta,30A(1974) 2005.
13. I. Sidis, Y.G. Sidir, M. Kumalar and E. Tasal, Ab initio Hartree-Fock and Density Functional Theory Investigations on the Conformational Stability, Molecular Structure and Vibrational Spectra of 7-Acetoxy-6-(2,3-dibromopropyl)-4,8-dimethylcoumarin Molecule, J. Mol.Structure.,964, 134-151(2010).
14. A Cavalli; X Salvatella; CM Dobson and M Vendruscolo, Proc. Natl. Acad. Sci. USA 2007, 104, 9615-9620.
15. N. Subramani; N. Sundriganesan and J. Jayabharathi Spectrochim.Acta A, 2010,76,259-269.
16. S Muthu; EI Paulraj, J.Chem.Pharm. Res.,2011,3(5),323-339.
17. N Sundaraganesan; H Uma Maheswari; B Dominic Joshua; C Meganathan; M Ramalingam, J. Mol. Structure (Theo chem.), 2008, 850,84-93.
18. G Varsanyi, Vibrational Spectra of Benzene Derivatives, Akademiai Kiado, Budapest, 1969.
19. S. Gunasekaran, S.R. Varadhan, K. Manoharan, Asian J. Phys. 2 (1993) 165.
20. S. Gunasekaran, R.K. Natarajan, R. Rathikha, D. Syamala, Ind. J. Pure Appl. Phys. 43 (2005) 503.
21. S. Ramalingam; S.Periandy; M. Govindarajan and S Mohan, Spectrochim.Acta Part A, 2010, 75, 1552-1558.
22. A.R. Krishnan et al./spectra chemical Acta part A 78(2011) 582-589.
23. M. Szafran, A. Komasa, E.B. Adamska, J. Mol. Struct. 827 (2007) 101-107.
24. R.G. Parr, R.A. Donnelly .M. Levy, W.E. Palke, J. Org.Chem. 67 (2002) 4747.

25. V.Arjunan et al., Spectrochem Acts Part A: Mol. Biomol. 96 (2012) 506-516.
26. K. Fukui, theory of orientation and stereoselection , Reactivity and Structure, Concepts in organic chemistry, Springer, Berlin (1975).
27. H. Abou-Rachid, Y. Song, A. Hu, S. Dudy, S. V. Zybin and W. A. Goddard, predicting solid-state Heats of Formation of Newly synthesized polynitrogen Materials by using quantum Mechanical Calculations, J. Phys. Chem. A., 112(46), 11914-11020 (2008).
28. Ahmed, A. B.; Feki, H.; Abid, Y.; Boughzala, H.; Minot, C. *SpectrochimicaActa Part A* 2010, 75, 293.

## Reference

- [1] T.L. Gilchrist, Heterocyclic Chemistry, 3th ed., Longman, Harlow, 1997, pp. 1-8.
- [2] J.A. Joule, K. Mills, Heterocyclic chemistry, fifth ed., Wiley Blackwell, Oxford, 2010, pp.645-664.
- [3] M. Balasubramanian, J.G. Keay, Compr. Heterocycl. Chem. II 5 (1996) 245-300.
- [4] C.DJohnson, Compr. Heterocycl. Chem. II 5 (1996) 1-35. 5. G. Jones, Compr. Heterocycl. Chem. II 5 (1996) 167-243.
- [5] S.P. Jose, S. Mohan, Spectrochim. Acta A 64 (1) ( 2006) 240.
- [6] Venkateswaran, S. On the Raman effect in liquid pyridine. J PhysChem 1930;34:145-52
- [7] Corrsin L, Fax BJ, Lord RC. The Vibrational Spectra of Pyridine and Pyridine-d<sub>5</sub>, J ChemPhys 1953; 21:1170-76.
- [8] Cook GL, Church FM. Correlations of the Infrared Spectra of some Pyridines. J PhysChem 1957;61:458-62].
- [9] Johnson TJ, Disselkamp RS, Su YF, Fellows RJ, Alexander ML, Driver CL. Gas-phase Hydrolysis of SOCl<sub>2</sub>: Implications for its Atmospheric Fate. J PhysChem A 2003;107:6183-90
- [10] R.P. Hirschmann, et al., Spectrochim. Acta A 30 (1974) 1293.
- [11] R. Ditchfield, Mol.Phys.27 (1974) 789. K. Wolinski, J.F. Hinton, P. Pulay, J. Am. Chem. Soc. 112 (23) (1990) 8251.
- [12] J .H.Vander Mass and E.T.G.Lutz, Spectrochimca Acta,30A(1974) 2005.
- [13] I. Sidis, Y.G. Sidir, M. Kumalar and E. Tasal, Ab initio Hartree-Fock and Density Functional Theory Investigations on the Conformational Stability, Molecular Structure and Vibrational Spectra of 7-Acetoxy-6-(2,3-dibromopropyl)-4,8-dimethylcoumarin Molecule, J. Mol.Structure.,964, 134-151(2010).
- [14]A Cavalli; X Salvatella; CM Dobson and M Vendruscolo, Proc. Natl. Acad. Sci. USA 2007, 104, 9615-9620.
- [15] N. Subramani; N. Sundraganesan and J. Jayabharathi Spectrochim.Acta A, 2010,76,259-269
- [16] S Muthu; EI Paulraj, J.Chem.Pharm. Res.,2011,3(5),323-339.
- [17] N Sundaraganesan; H Uma Maheswari; B Dominic Joshua; C Meganathan; M Ramalingam, J. Mol. Structure (Theo chem.), 2008, 850,84-93.
- [18] G Varsanyi, Vibrational Spectra of Benzene Derivatives, Akademiai Kiado, Budapest, 1969.
- [19]S. Gunasekaran, S.R. Varadhan, K. Manoharan, Asian J. Phys. 2 (1993) 165.
- [20] S. Gunasekaran, R.K. Natarajan, R. Rathikha, D. Syamala, Ind. J. Pure Appl. Phys. 43 (2005) 503.]
- [21] S. Ramalingam; S.Periandy; M. Govindarajan and S Mohan, Spectrochim.Acta Part A, 2010, 75, 1552-1558.
- [22] A.R. Krishnan et al./spectra chemical Acta part A 78(2011) 582-589.
- [23] M. Szafran, A. Komasa, E.B. Adamska, J. Mol. Struct. 827 (2007) 101-107.

- [24] R.G. Parr, R.A. Donnelly .M. Levy, W.E. Palke, *J. Org.Chem.* 67 (2002) 4747.
- [25] V.Arjunan et al., *Spectrochem Acts Part A: Mol. Biomol.* 96 (2012) 506-516.
- [26] K. Fukui, theory of orientation and stereoselection , *Reactivity and Structure, Concepts in organic chemistry*, Springer, Berlin (1975).
- [27] H. Abou-Rachid, Y. Song, A. Hu, S. Dudy, S. V. Zybin and W. A. Goddard, predicting solid-state Heats of Formation of Newly synthesized polynitrogen Materials by using quantum Mechanical Calculations, *J. Phys. Chem. A.*, 112(46), 11914-11020 (2008).
- [28] Ahmed, A. B.; Feki, H.; Abid, Y.; Boughzala, H.; Minot, C. *SpectrochimicaActa Part A* 2010, 75, 293.
- [29] M. J. Frisch, G. W. Trucks, H. B. Schlegel, G. E. Scuseria et al., Gaussian, Inc., Wallingford CT, 2009.